

## Supplementary Material

# **Bridging Controlled Network Microstructure and Long Wavelength Fluctuations in Silica-Poly(2-vinylpyridine) Nanocomposites: Experimental Results and Theoretical Analysis**

Yuxing Zhou<sup>1,2</sup>, Benjamin M. Yavitt<sup>3</sup>, Zhengping Zhou<sup>4</sup>, Vera Bocharova<sup>4</sup>, Daniel Salatto<sup>3</sup>, Maya K. Endoh<sup>3</sup>, Alexander E. Ribbe<sup>5</sup>, Alexei P. Sokolov<sup>4,6</sup>, Tadanori Koga<sup>3</sup>, Kenneth S. Schweizer<sup>1,2,7\*</sup>

<sup>1</sup>Department Materials Science and Engineering, University of Illinois, Urbana, IL 61801

<sup>2</sup>Materials Research Laboratory, University of Illinois, Urbana, IL 61801

<sup>3</sup>Department of Materials Science and Chemical Engineering, Stony Brook University, Stony Brook, NY 11794

<sup>4</sup>Chemical Sciences Division, Oak Ridge National Laboratory, Oak Ridge, TN 37831

<sup>5</sup>Department for Polymer Science & Engineering, University of Massachusetts, Amherst, MA 01003

<sup>6</sup>Department of Chemistry, University of Tennessee, Knoxville, TN 37996

<sup>7</sup>Department of Chemistry, University of Illinois, Urbana, IL 61801

## A. Experimental

Figure S1 shows the raw intensity SAXS data, while Fig. S2 shows the dilute limit that serves as the form factor to convert intensity to structure factors. Figure S3 compares the nanoparticle structure factors at two temperatures; very little difference is observed. Moreover, differences between the structure factor at different temperatures at low  $q < 0.008 \text{ \AA}^{-1}$  are *not* conclusive due to instrumental resolution limitations. However, the existence of the upturn for the 27% NP loaded sample is robust and statistically significant.

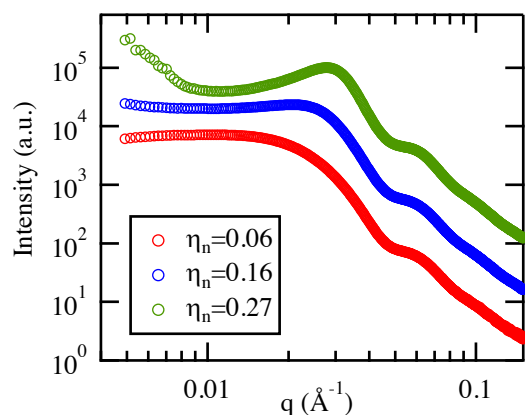


**Figure S1.** SAXS profiles  $I(q)$  (vertically shifted for clarity) for  $\eta_n = 0.06, 0.16$ , and  $0.27$  at  $T = 180 \text{ }^\circ\text{C}$ .

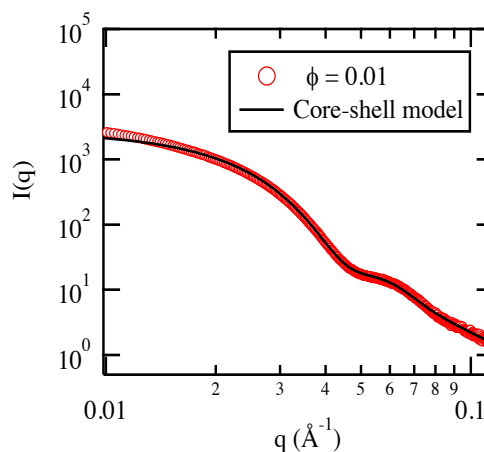


**Figure S2.** SAXS profile for  $\eta_n = 0.01$  at  $T = 180 \text{ }^\circ\text{C}$ . The solid line shows fit to a core-shell particle form factor with a Gaussian core size distribution.

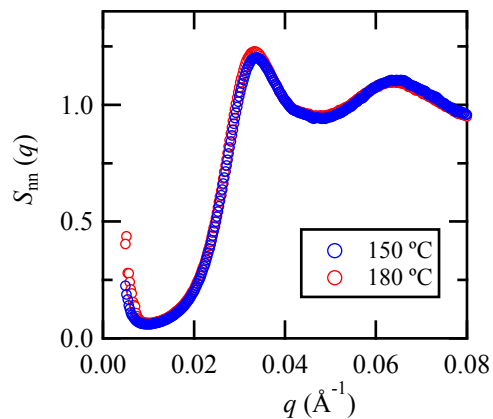


**Figure S3.** Representative temperature dependence of  $S_{nn}(q)$  for  $\eta_n = 0.27$ .

## B. Theoretical

### 1. Comparison between experimental and theoretical $S_{nn}(q)$

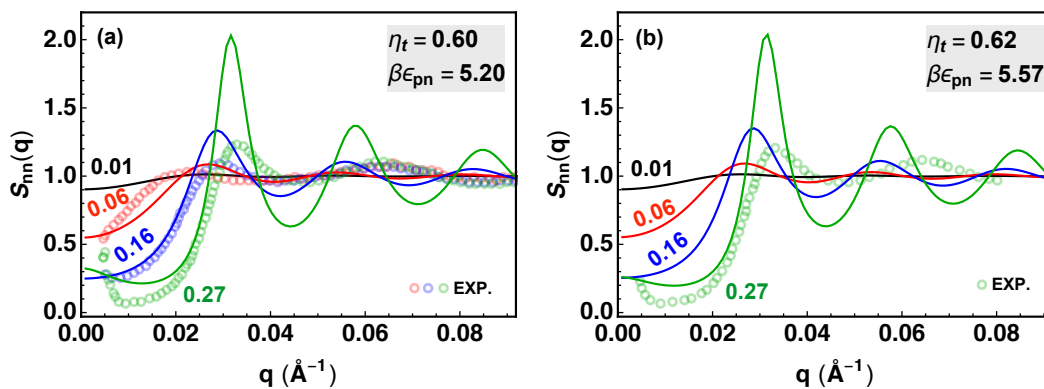


**Figure S4.** Same as Fig. 4 in the main text but with experimental results from Fig.2a (open circles) overlaid for comparison.

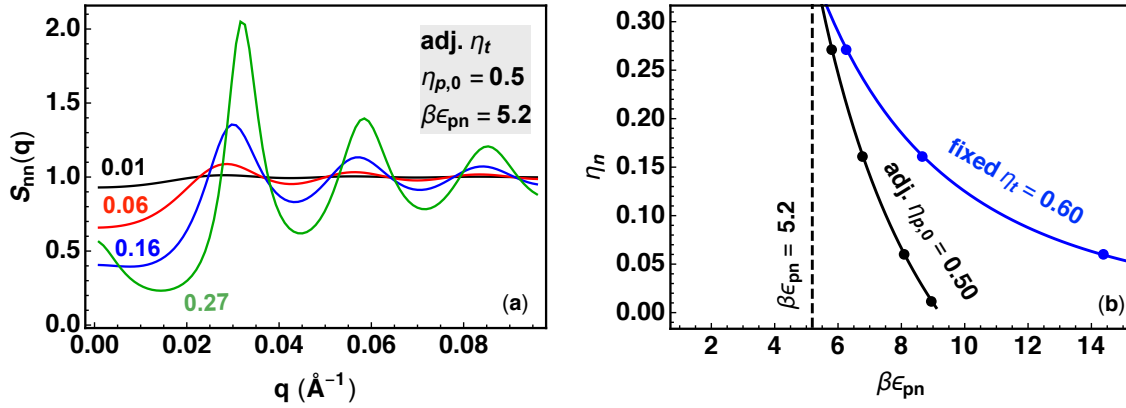


**Figure S5.** (a) NP-NP structure factor with adjusted total packing fraction. (b) Comparison of the bridging spinodal boundary predicted based on fixed  $\eta_t$  and adjusted  $\eta_t$  models.

## 2. Adjusted Packing Fraction Model

Figure S5 shows theoretical results analogous to Figs. 3c and 4 in the main text based on the adjusted packing fraction model defined by Eq. (5).

## 3. Effective Hard Sphere Model

Here we naively map NPs to hard spheres with an effective diameter that includes an experimental estimate<sup>1</sup> of the thickness of an adsorbed immobilized polymer shell on a SiO<sub>2</sub> NP of  $\sim 3\text{--}4$  nm. This implies a ratio of effective to bare NP diameter of  $\sim 1.35$ , and thus an effective packing fraction ratio of  $\eta_{HS}/\eta_n \sim 2.4$ . In our calculations we employ  $\eta_{HS}/\eta_n \sim 2.2$ , which is theoretically motivated by the PMF in the dilute NP loading case (see Fig. 5) where at  $r^*/\sigma \sim 13$  the barrier first exceeds  $\sim 2k_B T$  as two particles approach each other, so that  $r^*/d = 1.3$  and hence  $\eta_{HS}/\eta_n \sim 2.2$ . As a result, the bare  $\eta_n = 0.01$  to  $0.27$  are mapped to  $\eta_{HS} = 0.022$  to  $0.594$ . The results are shown in Fig. S6. We find, not surprisingly, this  $S_{HS}(k)$  is qualitatively different from the PNC  $S_{nn}(k)$  predicted by PRISM theory. For example,  $S_{HS}(0)$  is much too

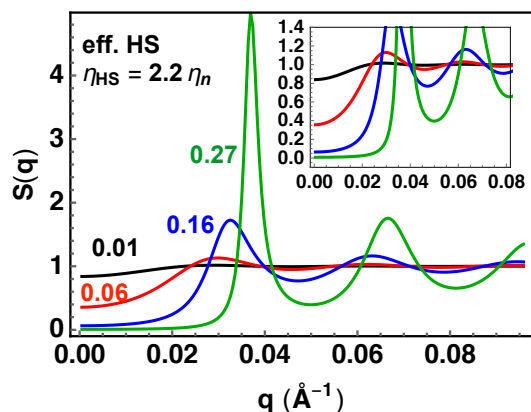


**Figure S6.** Nanoparticle structure factors for the mapped effective hard sphere fluid model.

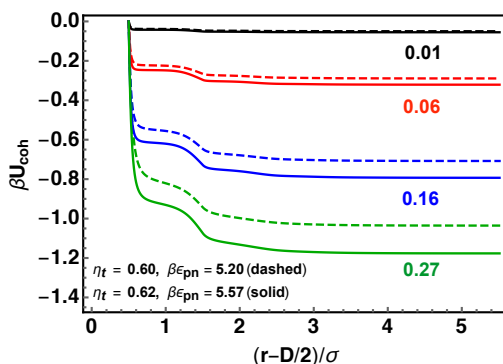


**Figure S7.** Cumulative cohesive energy density in units of thermal energy as a function of distance from the NP surface for parameters relevant to the silica-P2VP PNC at 180 and 150 °C.

small and the cage peak is much too large, and there is no upturn or curve crossing a low wavevectors for high loadings.

#### 4. Interfacial Cohesive Energy Density

The cohesive energy density in Eq. (6) can be expressed in a cumulative or spatially-resolved representation corresponding to the upper limit in the integration being a running variable  $r$ . Fig. S7 shows calculations of this quantity. Convergence is largely achieved at a

distance of 2-3 polymer segment diameters from a NP surface, as expected given the short range nature of the segment-NP attractive interaction.

## References

- (1) Griffin, P. J.; Bocharova, V.; Middleton, L. R.; Composto, R. J.; Clarke, N.; Schweizer, K. S.; Winey, K. I. Influence of the Bound Polymer Layer on Nanoparticle Diffusion in Polymer Melts. *ACS Macro Lett.* **2016**, 5 (10), 1141–1145.